UNIVERSITY OF OKLAHOMA

GRADUATE COLLEGE

EVALUATION OF FUNCTIONALITY AND SERVICE LIFE OF
ULTRA-HIGH PERFORMANCE CONCRETE LINK SLAB CONNECTIONS FOR BRIDGES

A THESIS

SUBMITTED TO THE GRADUATE FACULTY

in partial fulfillment of the requirements for the Degree of

MASTER OF SCIENCE

CIVIL ENGINEERING

By

CLAY REED
Norman, Oklahoma
2022
EVALUATION OF FUNCTIONALITY AND SERVICE LIFE OF
ULTRA-HIGH PERFORMANCE CONCRETE LINK SLAB CONNECTIONS FOR BRIDGES

A THESIS APPROVED FOR THE SCHOOL OF CIVIL ENGINEERING AND
ENVIRONMENTAL SCIENCE

BY THE COMMITTEE CONSISTING OF

Dr. Jeffery Volz, Chair

Dr. Royce Floyd

Dr. Shreya Vemuganti

Acknowledgements

Thank you to my advisor, Dr. Jeffery Volz, for approaching me with this wonderful opportunity and providing relentless patience and guidance. Thank you to Dr. Royce Floyd and Dr. Shreya Vemuganti for their guidance and support as committee members. Thank you to my research team and everyone at Fears Lab for their ample assistance, with special thanks to the lab manager, John Bullock, as well as Jack Heiser, Jorge Vargas, Jacob Choate, Trevor Looney, and Stephen Roswurm.

Thank you to all of my friends and family for their unwavering support, including those previously mentioned. This research and thesis would not have been possible without their love and motivation throughout.

Abstract

Structural longevity and sustainability are rising priorities in bridge construction. Accelerated bridge construction is a response to such a demand, with a goal of providing bridges with a longer service life in a construction process more time and cost effective. Link slabs have been an attractive alternative to expansion joints by providing protection for rebar and underlying reinforcement from contaminant exposure. Traditionally constructed with conventional concrete, these bridge connections are still porous and susceptible to corrosion, though at a slower rate than expansion joints. There is a growing interest in ultra-high performance concrete (UHPC) in bridge construction due to its higher strength and durability. Utilizing UHPC in link slabs has the potential to further extend the service life of these connections and mitigate the frequency of costly repairs and replacements.

Using a non-proprietary UHPC mix developed at the University of Oklahoma, labeled "J3," this research investigated its performance as a link slab construction material. The UHPC's performance was compared to Class AA concrete, the Oklahoma Department of Transportation (ODOT) conventional mix standard for bridge deck construction. Both materials were used in constructing link slab specimens, with segments of these specimens subjected to durability and corrosion tests. A link slab of each concrete mix experienced cyclic loading prior to segmentation and durability testing. This provided insight to how in-service loading may affect the connection's performance compared to a newly-constructed link slab. Tests conducted included rapid freeze-thaw cycling and accelerated corrosion testing.

Results were based on physical observations and measuring resonant frequencies for a Relative Dynamic Modulus (RDM) for each specimen throughout 350 freeze-thaw cycles. Accelerated corrosion testing was conducted to determine the concretes' ability to withstand corrosion to rebar within link slabs. Rebar conditions were observed after 5 weeks and 9 weeks of corrosion testing. UHPC specimens, pre-loaded or not, resisted loss of strength after 350 freeze-thaw cycles better than conventional concrete, with the majority of UHPC specimens having RDM readings higher than 100%, which implies a strength/durability gain during testing. Loading did slightly influence the UHPC mix's performance but had a greater impact on the performance of the Class AA mix. Corrosion observations show the effects of testing were significantly more severe for conventional concrete, resulting in discoloration and oxidation on rebar and the surrounding concrete for both loading conditions. UHPC results are far more promising, with no signs of damage due to corrosion on or around the rebar, with prior loading conditions having virtually no influence on these results. Overall, UHPC proved to be a superior construction material for link slabs by providing greater resistance to temperature effects and greater protection for reinforcement, offering a longer service life with fewer repairs.

Table of Contents

List of Tables

List of Figures

xiii

1. Introduction

1.1 Background

Bridge joints allow longer bridges to be built by connecting adjacent segments into one continuous span. These longer bridges provide safe travel over rivers, lakes, and even other roads. Traditional connections, such as expansion joints, have small spaces between the concrete sections to allow free expansion and shrinkage. Steel coverings and silicone or rubber seals are placed over these gaps to give traffic a smoother ride but fail to protect the connection. Even with a sealant present, contaminated water can seep into substructure elements. This exposure shortens the service life of the joint and can cause more frequent repairs and even replacements. With a call to minimize costs and time in bridge construction and maintenance, deck connections known as link slabs are utilized in place of traditional bridge joints. Link slabs provide a more thorough covering for the substructure, requiring fewer repairs. However, this connection has traditionally been constructed with conventional concrete, which is porous and can crack. These properties leave the bridge structure and substructure susceptible to performance issues and deterioration over time.

A potential alternative material in link slab construction is ultra-high performance concrete (UHPC). Compared to conventional concrete, UHPC has higher compressive and tensile strengths, as well as excellent bond strength to other materials, especially concrete. Though this

material has been utilized in practice, its use in link slab construction will benefit from more research.

The research detailed and discussed in this document examined the performance of a UHPC link slab under service loading and deterioration. Two UHPC link slabs were constructed connecting slab sections, with one subjected to cyclic load testing and both exposed to freeze-thaw and accelerated corrosion testing. Two link slabs of conventional Class AA ODOT concrete were constructed and tested similarly as control specimens. With UHPC utilized in link slab construction, the system can have the potential to provide a more secure connection requiring less time and money in repair and replacement costs.

1.2 Project Scope

The focus of this research was to determine the performance of UHPC link slabs during service life conditions, namely durability and corrosion. To determine how UHPC performed compared to conventional concrete, link slab segments of both materials were subjected to rapid freeze-thaw cycling and accelerated corrosion testing. In preparation of these tests, some of the specimens were loaded cyclically to represent in-service link slabs. This variation in specimens provides insight on how each concrete performs not only as a newly-construction link slab but as a connection exposed to service load conditions as well.

1.3 Objectives and Goals

The following subsections cover the objectives and goals guiding this research study.

1.3.1 Objectives

The main objective for this research was to compare the performances of conventional (Class AA ODOT) concrete and UHPC as link slab connections subjected to accelerated corrosion and freeze-thaw testing. Both forms of concrete were examined during the four following states: corrosion with no loading, corrosion with pre-loading, freeze-thaw with no loading, and freeze-thaw with pre-loading. Cracking and any other effects observed throughout all testing were studied. Results will reflect whether UHPC is a viable or better option for link slab connections in bridge decks.

1.3.2 Goals

The main goal for this research was to obtain performance results for both conventional concrete and UHPC as a link slab connection material. These results will be used to help prepare a service life design guide for UHPC link slabs.

1.4 Outline

This thesis consists of six chapters and one appendix. Chapter 1 provides a brief background and justification for the study, as well as an outline of the scope, objectives, and goals of the research. Chapter 2 examines literature relevant to the scope of the conducted research, including information on link slabs, UHPC, and why research is necessary. Chapter 3 covers the specimen

fabrication and cyclic loading of the specimens. Chapter 4 summarizes the procedure and conduction of rapid freeze-thaw cycling, along with the results; Chapter 5 provides the same information for accelerated corrosion testing. Chapter 6 includes a summary of the findings of all tests, conclusions drawn from these observations, and recommendations for future research. Supplementary tables and figures are included in the appendix followed by a list of references.

2. Literature Review

2.1 Overview

This chapter covers the review of literature relevant to the topics of this research. This includes a description of expansion joints and link slabs, as well as the former's issues and how they are mitigated with the latter. Accelerated bridge construction is discussed with how link slabs help to achieve goals the construction pursues. Ultra-high performance concrete (UHPC) is explained as a construction material and how its properties can further improve link slabs. Reviews of previous research regarding test methods used in this research and UHPC as a link slab bridge joint construction material are also included.

2.2 Bridge Joints

The traditional way to construct bridges consisting of more than one segment is to connect them with expansion joints. These joints allow for adjacent decks and girders to expand or shrink independently of each other due to thermal changes, preventing internal cracking in the decks. There are variations used to build bridges around the world, but all forms span the entire width of the connected sections. This connection joins the entire depth of the deck, with the deck and girders of simple-span bridge sections fully bonded. This causes the connection to behave as an end roller; with no moment in the connection, each span is allowed to behave as a simple span (Azizinamini et al., 2013). An example cross-section of an expansion joint is shown in Figure 2-1 (Haikal et al., 2019). This method presents issues affecting the service lives of their respective

structures, particularly as interior connections. Expansion joints often include only sealant with the deck slab ends having steel covers. This leaves the interior of the connections vulnerable to contaminated water seepage, even with a joint seal. When contaminated water seeps into the bridge decks, it exposes reinforcing steel and the concrete faces of the connected spans. This contact results in prematurely corroding the reinforcing steel, cracking the concrete, and the concrete-steel bond deteriorates within the bridge deck as well as beam ends and piers (Wang et al., 2017). These setbacks shorten the service life of a bridge and require repairs earlier than anticipated. Simple repairs do not resolve the initial problems, but instead result in more frequent and costly repairs.
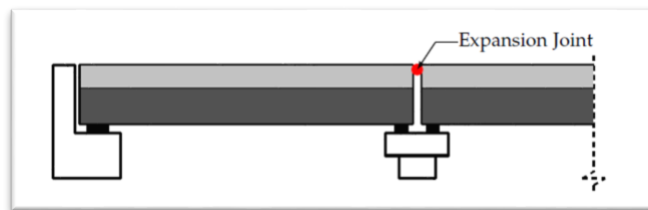
Figure 2-1: Expansion joint example (Haikal et al., 2019)

2.3 Link Slabs

An alternative to installing an expansion joint between two bridge decks comes in the form of link slabs. Like expansions joints, they span the entire width of the sections they connect. Link slabs connect adjacent spans by only the bridge decks. This creates a continuous, jointless deck above separate girders. With girder ends independent from the connection through debonding, their behavior as separate simple-span ends is maintained (Azizinamini et al., 2013). An example cross-section of a link slab joint is shown in Figure 2-2 (Haikal et al., 2019).
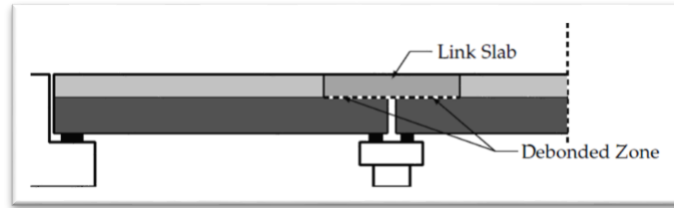
Figure 2-2: Link slab joint example (Haikal et al., 2019)

Concrete is a common construction material for link slabs, providing a more secure seal from outside contaminates for bridge decks than expansion joints. With the concrete connection, any changes in temperature within the bridge can be transferred throughout the structure. The design of this connection varies internationally and even from state to state within the United States. Figure 2-3 shows a cross-section of one of the designs the New York Department of Transportation (NYDOT) has developed (Scarlata, 2017). Link slabs require less frequent repairs due to corrosion within the bridge deck, beam, and substructure. For these reasons, interest in link slab connections has increased.
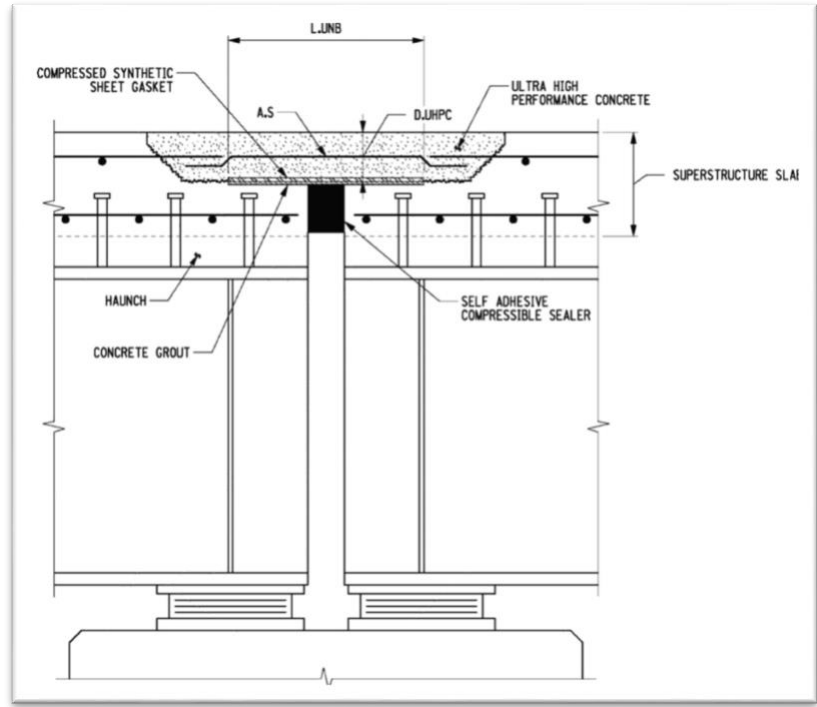
Figure 2-3: Link Slab Design Example (Scarlata, 2017)

2.4 Accelerated Bridge Construction

Constructing and maintaining bridges is extremely costly. Bridge repairs in particular result in expensive losses with road traffic disruptions. To speed up the process of repairing or replacing bridge components, a means was developed known as Accelerated Bridge Construction (ABC). Through advanced scheduling and accelerated methods of construction, ABC helps minimize economic losses brought on by prolonged traffic obstructions. The attraction of mitigating unnecessary loss has influenced Departments of Transportation across the United States, including Oklahoma's (ODOT), to adopt this method for some cases.

8

With their easy and rapid means of construction, link slabs are an ideal choice for simple-span connections when utilizing ABC. Replacing expansion joints with link slabs can be a viable option in dealing with interior joints in need of repair (Shafei et al., 2018). Not only are the connections repaired, issues of expansion joints are also eliminated, leaving the bridge in better shape than when it was initially constructed. Link slabs also allow thermal changes to transfer axially between the connected spans. This helps prevent isolated wear on a section of the bridge due to excessive heating or cooling. Unfortunately, link slabs created with conventional concrete are porous and still susceptible to cracking and seepage.

2.5 Ultra-High Performance Concrete

A relatively new construction material known as ultra-high performance concrete (UHPC) has been on the rise in interest for field applications. Developed in the 1990s, UHPC has been used as a superior repair material compared to conventional concrete. Many properties of UHPC, including compressive strength and viscosity, differ from those of conventional concrete mixes, often benefiting the former's performance. Like conventional concrete mixes, UHPC contains portland cement, fine aggregate, and water but no coarse aggregate. In addition, UHPC typically includes silica fume, high-range water reducing admixture (HRWR), and discrete reinforcement, such as steel fibers (Russell and Graybeal, 2013). UHPC can be defined as "cementitious-based composite materials with discontinuous fiber reinforcement" and typically has compressive strengths greater than 20 ksi (Russell and Graybeal, 2013). The steel fibers present in UHPC are a major contributor to its strength, especially in tension.

Other properties of UHPC make it a superior alternative to conventional concrete when constructing link slabs. The absence of larger aggregate in UHPC and chemical makeup and particle distribution of its mixture accounts for higher flowability than conventional concrete, thus allowing easier application. For link slab construction, UHPC's ability to create a stronger bond to reinforcement than conventional concrete allows for a smaller connection design. The use of fine aggregates helps create a less porous product, delivering an even tighter seal than conventional concrete against water seepage into the bridge deck. Even if contamination manages to seep into the bridge deck, the small quantity of corrosive material and higher compressive strength expected of the UHPC will minimize corrosion (Abosrra et al., 2011). This provides the best protection of any connection discussed so far.

Despite the advantages of UHPC, there are a couple major points dissuading a more universal use. Due to its tendency to quickly lose flowability, it is not ideal to mix and pour UHPC in large batches, as practiced with conventional concrete. The composition of UHPC causes it to be more expensive, as most mixtures are proprietary. Though there have been steps to develop non-proprietary mixtures (Floyd et al., 2018), the price can still be an issue. It is imperative the research on the beneficial performance of UHPC is conducted to further push the desire to make UHPC more accessible.

2.6 Previous UHPC Link Slab Research

Research examining UHPC as a connection material is relatively new, with the most substantial amount occurring within the last decade. While some research looks at many types of

connections UHPC can be used for (Graybeal, 2014; Floyd et al., 2018), information on using it to construct link slabs is limited not only by quantity in literature but by consistency in design. This includes differences in slab end shape, reinforcement in the link slab, and depth of the connection.

Even scarcer are testing of UHPC link slab connections under cyclic loading. This is a major concern for bridge construction, which is subjected to cyclic loading through traffic. A recent study at the University of Oklahoma (Chea, 2020) tested a UHPC connection resembling a link slab under cyclic loading, showing UHPC provided even more strength than predicted. However, there was only one type of connection design used in testing – a fully bonded full joint T-shaped connection. This resulted in the connected slabs behaving as a continuous span across the link slab, with moments able to transfer between the sections. Results may have differed if an alternate design was used or if the joint was partially debonded from the slabs, behaving as more of a pinned connection. These variables call for more testing to establish a more thorough understanding of UHPC as a link slab connection material.

3. Specimen Construction and Preparation

3.1 Scope of Work

This research examines the effects of service loading on link slab connections when subjected to accelerated corrosion and freeze-thaw testing. The primary materials used to construct the test specimens were conventional concrete and UHPC. The following chapter will cover the preparation and construction of the four link slab specimens, two of each material. This involves constructing individual concrete slabs before joining them with the connections of interest and applying cyclic loading to one of each specimen type. All fabrication was conducted at the Donald G. Fears Structural Engineering Lab (Fears Lab).

The final outer dimensions of a specimen were 6 ft. by 8 ft. in plan and 8 in. in thickness. Figures 3-1 through 3-3 show the details of a fully constructed link slab specimen. Note the 2-in.-thick gap between the connected slab sections allowing them to behave independently of each other. All slab sections were constructed of conventional concrete with the connection being of either conventional concrete or UHPC. This link slab design is based on the design developed and adopted by the New York State Department of Transportation (NYDOT) for UHPC.
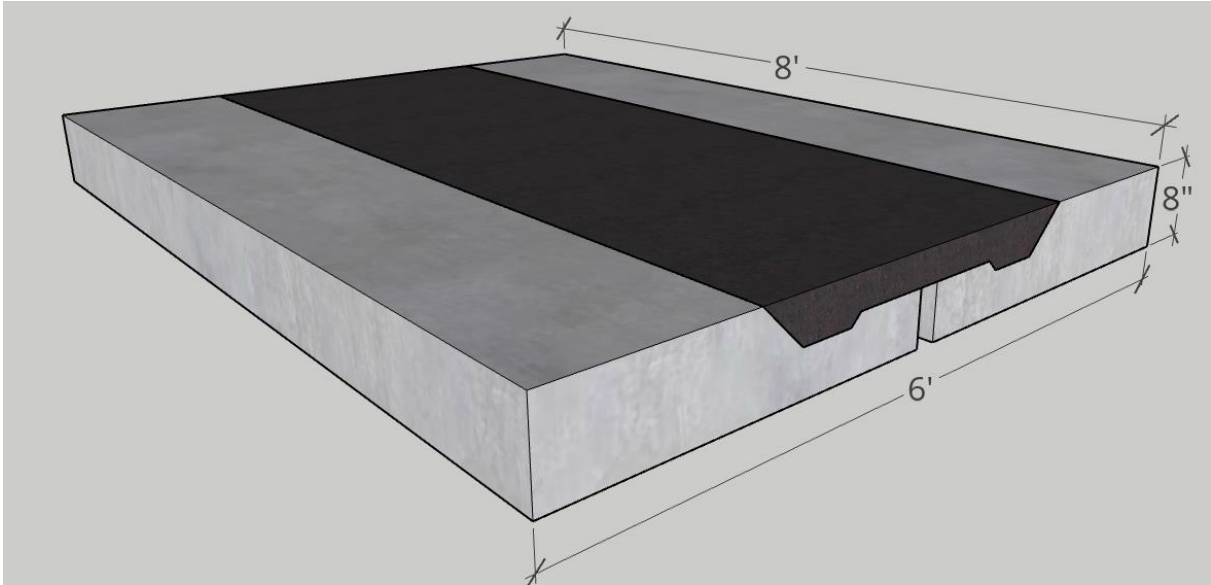
Figure 3-1: Link slab specimen design
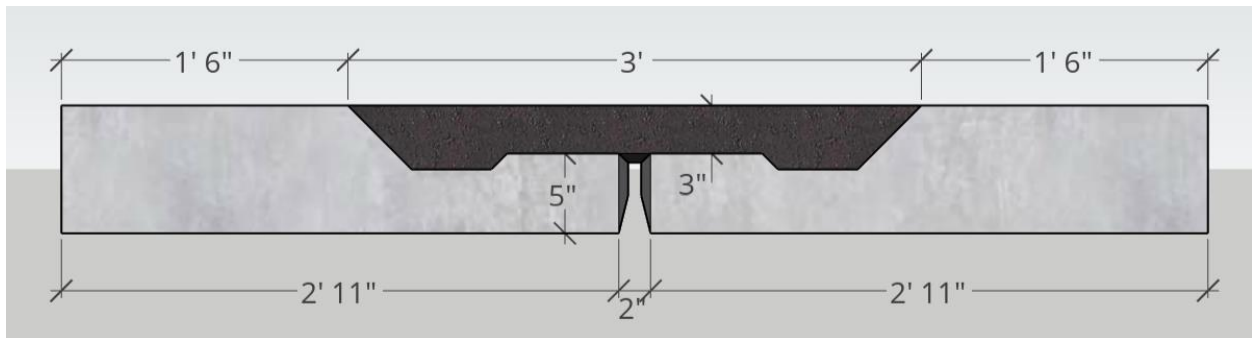
Figure 3-2: Link slab specimen end elevation

13
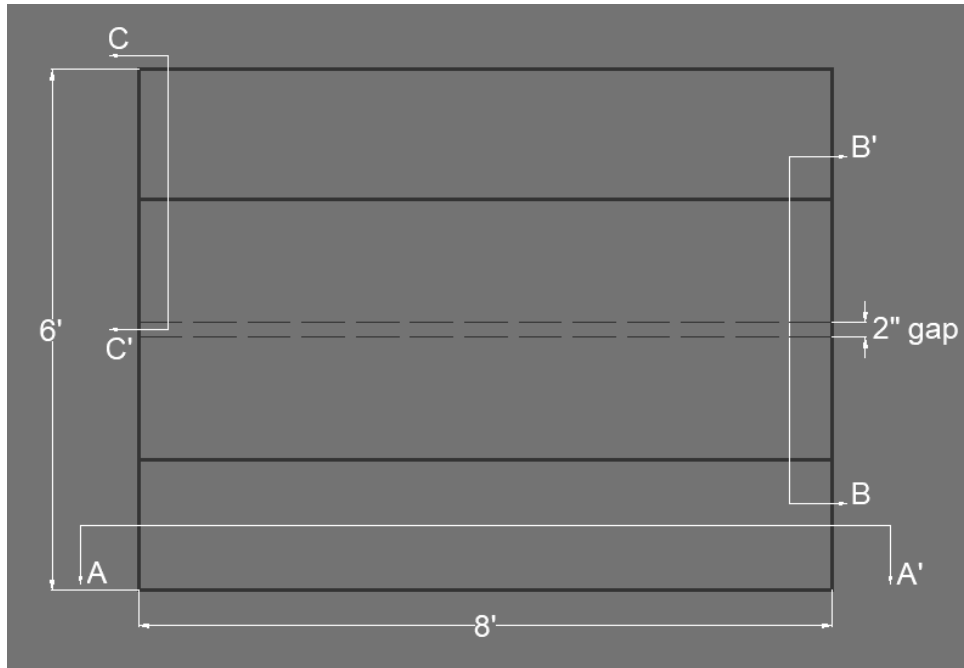
Figure 3-3: Plan view of specimen design (section marks refer to later figures)

3.2 Class AA Deck Slabs

Each of the four specimens required two slabs to serve as the connected bridge joints. Four

wooden forms were fabricated to facilitate the construction of two concrete slab sections each,

for a total of eight slab sections. The inner dimensions of each form were 96 in. by 35 in. in plan

and 8 in. in thickness. Before each casting, the forms were prepared with silicone along the

interior edges and form release on all surfaces to be in contact with concrete. Formwork, before

rebar or inserts were installed, is shown in Figures 3-4 and 3-5.

Figure 3-4: Formwork for one slab

Figure 3-5: Formwork for four slabs

To create the connection design, a foam insert was constructed and placed in each section. Each foam section spanned the entire 8 ft. length. Figure 3-6 provides the dimensions for the insert's uniform cross-section, with all non-right angles at 45 degrees. Figures 3-7 and 3-8 show the finished cross-section of one of the inserts. These connection dimensions are based on the NYDOT link slab design reported in the literature review. One insert was placed in each form along one side of the 8 ft. length with the 17 in. side face down and the larger slope facing into the form. The placement was the same for all slab sections. Holes were drilled into the slanted face of the foam to insert rebar extending out of the concrete, which is shown in Figure 3-8.
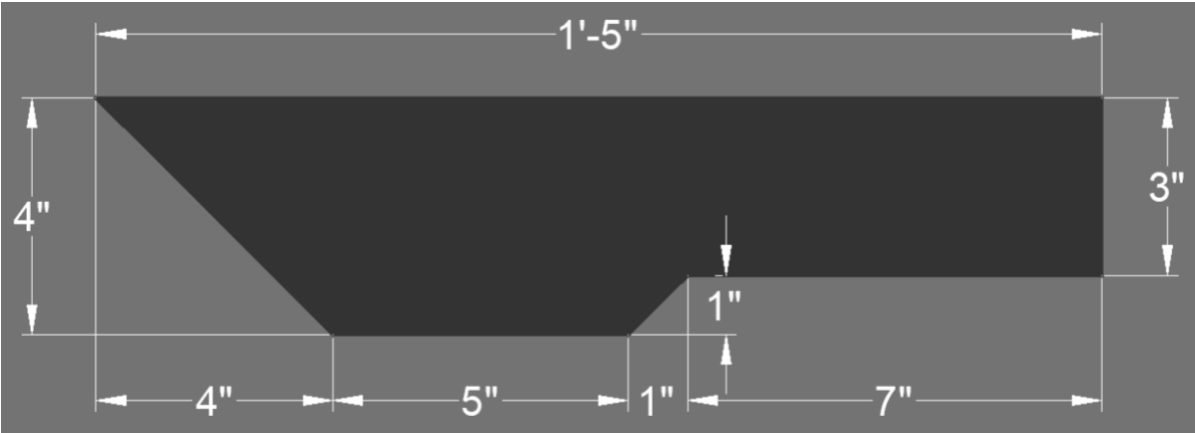
Figure 3-6: Foam insert cross-section

Figure 3-7: Connection cavity foam insert cross-section

Figure 3-8: Foam insert with drilled holes for rebar

For each slab section, #5 Grade 60 rebar was cut and tied into two reinforcing layers to ensure any failure that may develop during cyclic loading would occur in the link slab. Cover was 1.5 in. from the section top and bottom based on the requirements of ACI 318 and 1 in. at rebar ends. The plans of these layers are included in Figures 3-9 through 3-12.
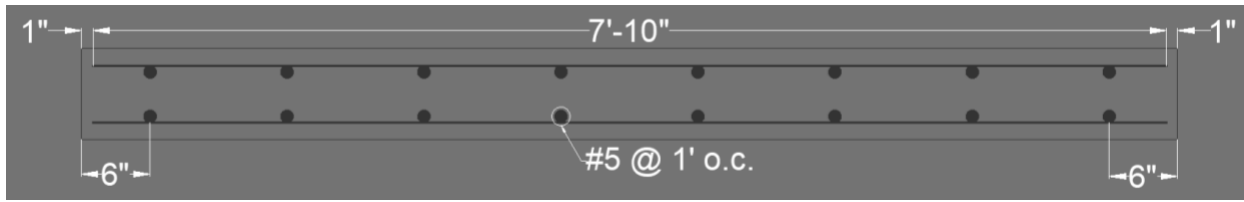
Figure 3-9: A-A' elevation of specimen design from Figure 3-3
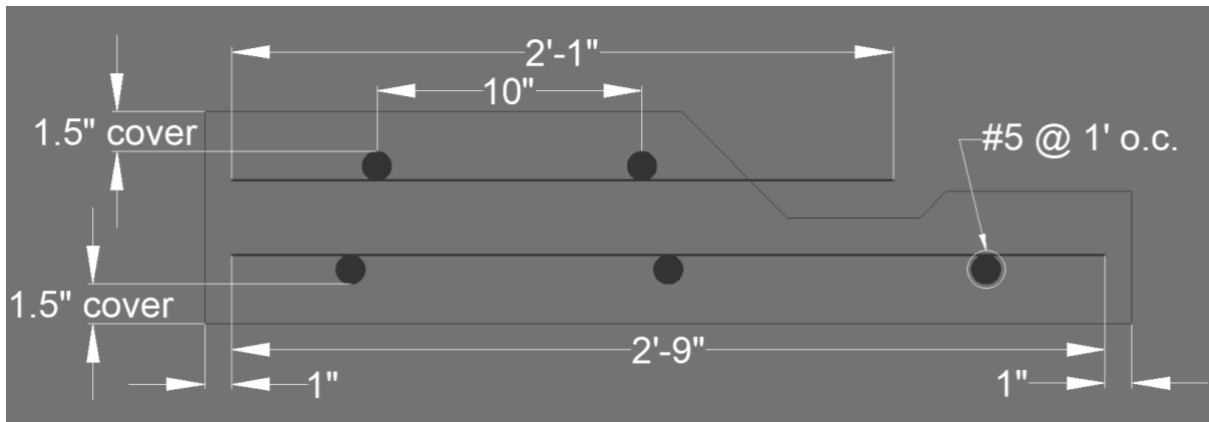
Figure 3-10: B-B' elevation of specimen design from Figure 3-3
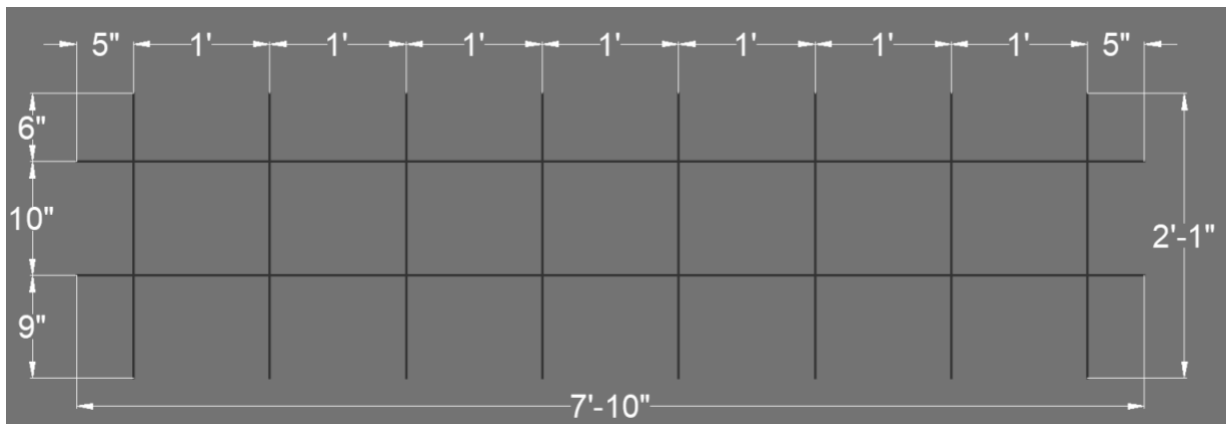
Figure 3-11: Slab section rebar cage top layer, all size #5

18
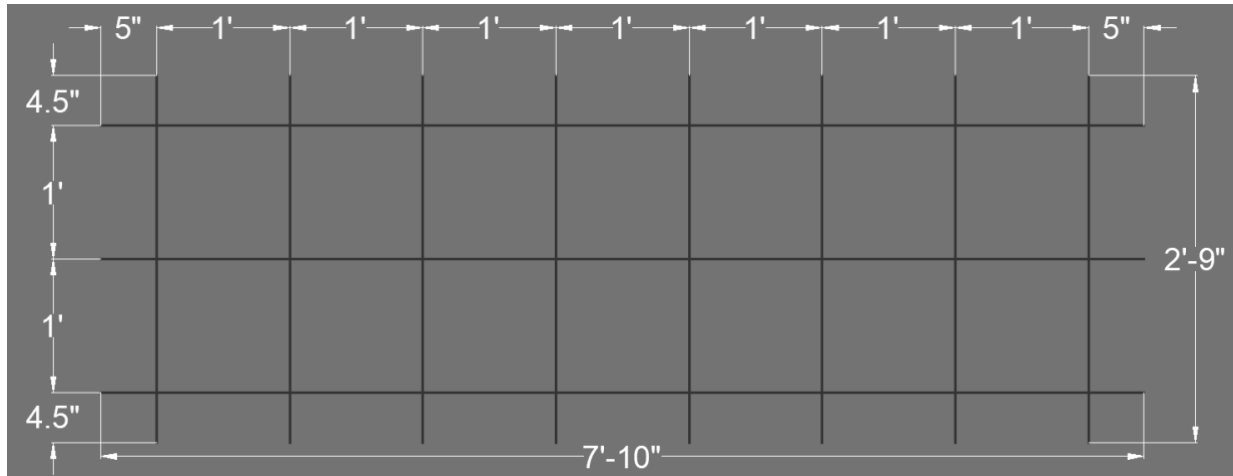
Figure 3-12: Slab section rebar cage layout bottom layer, all size #5

To facilitate casting the desired link slab connection for this research, all slab segments were cast upside-down. The top rebar cage layer was installed first along with the foam insert (Figure 3-13) followed by the bottom rebar cage layer (Figure 3-14). Each cage layer was tied prior to being placed. To move these slabs once they have cured, two all-thread bars were installed on each short face of the slab specimen, with four bars total per section. The all-thread was cut to 18 in. and extended 4 in. out of the formwork at a height of 4 in. above the slab face. These bars were tied to the existing rebar and are shown in Figure 3-14.

In the event these decks were cast in place, a more substantial insert would be needed to create the desired connection and withstand the upward forces of the concrete underneath as it was being poured. It would also need the ability to be removed before installing the link slab. Considering the rebar extensions protruding from the deck, a reusable insert capable of preventing leaks around the exposed rebar is ideal.

19

Figure 3-13: Slab formwork with foam insert and "top" rebar cage layer

Figure 3-14: Slab formwork with all rebar, all-thread installed

There were two rounds of concrete pours, each producing four slab sections. For each round, all

slabs were cast using a Class AA ODOT concrete mix, the state standard for bridge deck

construction (for conciseness, this mixture will be referred to as "AA" moving forward). This

mixture was provided by a ready-mix concrete supplier for all eight slab sections. Figure 3-15

shows a set of slabs right after casting. All slabs were left in their forms to cure with wetted

burlap on the exposed surface for seven days. After seven days, the sections were released from

the forms and flipped over to their testing orientation, as shown in Figure 3-16. The foam was

stripped from the connection cavity to expose the rebar to be used for splicing (Figure 3-17). The

foam left smoother concrete surfaces than anticipated, so these surfaces were sandblasted prior to placing the link slab concrete. This provided a rough texture to promote a better bond for the connection pour.

Figure 3-15: Set of slab sections after pouring, screeding

Figure 3-16: Slab sections after demolding, flipping

Figure 3-17: Slab sections with foam removed

23

3.3 Class AA and UHPC Link Slab Joint

Slabs were paired and oriented with the link slab connection block-outs facing each other, as shown in Figure 18. Two inches separated the outside edges of the connections to allow independent behavior of each slab section during cyclic load testing. A strip of wood or steel tube was used as a divider and ran the entire length of the connection to maintain the spacing and bridge the section gap. Formwork was also placed on the connection ends to prepare for the link slab pour, as shown in Figure 3-18. The level surface created across the gap is where the bond breaker was installed. A compressed synthetic sheet gasket was used as the bond breaker, the same material used by NYDOT, where this link slab design was developed. A small amount of silicone was used to hold the sheet in place during casting. This is shown in Figure 3-19, with concrete cylinders acting as weights to hold the gasket sheet in place while the silicone sets.

Figure 3-18: Connection preparation with divider, formwork installed

Figure 3-19: Connection preparation with sheet gasket installed

The exposed rebar of the connected sections was spliced to their mirroring bar with #5 Grade 60 rebar. Each splice was sectioned to have 4 in. of overlap on either side. For each connection, three splicing bars had a copper wire soldered to them in preparation for corrosion testing (Figure 3-20). Transverse #4 Grade 60 rebar was placed and tied above the spliced rebar, spaced 8 in. on center. Dimensions are included in Figures 3-21 and 3-22. The cover was 1.5 in. from the top face based on ACI 318 requirements. Figure 3-23 shows a fully-prepped specimen ready for casting.

Figure 3-20: #5 rebar soldered with copper wire
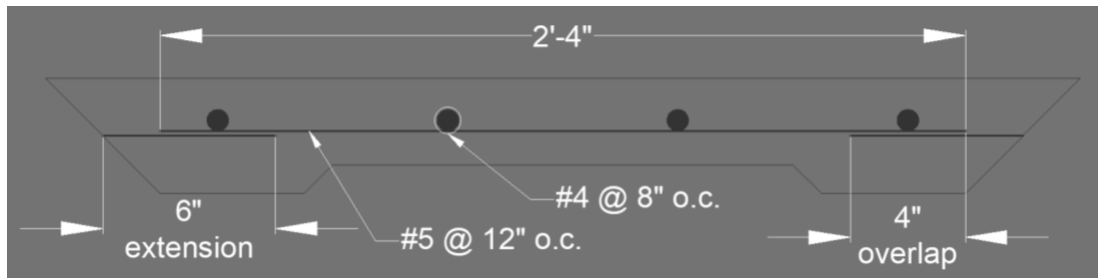
Figure 3-21: C-C' elevation of specimen design from Figure 3-3
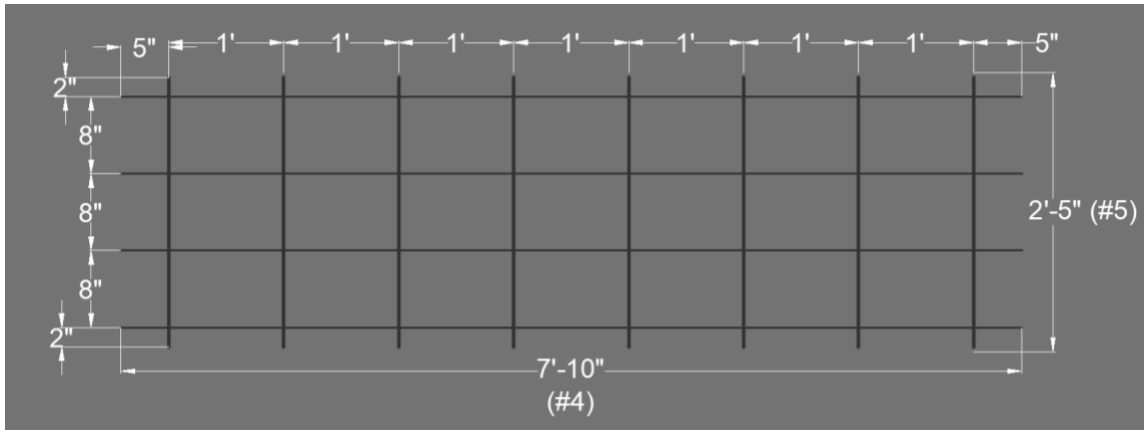
Figure 3-22: Connection rebar cage layout

Figure 3-23: Connection fully prepped for casting

There was a total of four link slab joints poured: two consisting of the same Class AA mix used for the slab segments and two consisting of the J3 non-proprietary UHPC mix. The "J3" simply refers to the UHPC mix design used in this research and will be used interchangeably when referring to UHPC. Tables 3-1 and 3-2 detail the mix designs for AA and J3, respectively. All

27

connection mixes were batched, mixed, and poured at Fears Lab. After their respective pours, both the J3 and the AA mix were left to cure for 28 days. Figure 3-24 shows one of the AA link slabs immediately after it was poured and leveled off. All joints were covered with wet burlap for the first seven days of curing.

Table 3-1: Design material quantities for ODOT Class AA concrete

Material	Quantity
Type I Cement	588 lb/yd^3
Coarse Aggregate	1857 lb/yd^3
Fine Aggregate	1264 lb/yd^3
Water	223 lb/yd^3
Air Entrainer	122 mL/yd^3
High-Range Water Reducer (HRWR)	522 mL/yd^3

Table 3-2: Design material quantities for J3 mix UHPC, 2% steel fibers

Material	Quantity
Type I Cement	1180 lb/yd^3
Masonry Sand	1966 lb/yd^3
Ground Granulated Blast-Furnace Slag (GGBFS)	590 lb/yd^3
Silica Fume	197 lb/yd^3
Steel Fibers	265 lb/yd^3
Water	393 lb/yd^3
High-Range Water Reducer (HRWR)	12791 mL/yd^3

Figure 3-24: Class AA link slab after pouring, leveling

3.4 Tabulating Specimens

Going forward, a tabulated shorthand may be used to concisely distinguish each connection and their respective specimens for testing. The first part of a label will identify what material the specimen is: "AA" for the Class AA ODOT concrete, "U" for the UHPC J3 mix. The latter portion of the identifier is separated with a hyphen and provides the specimen's loading condition: "L" for loaded prior to durability testing, "N" for no prior loading. For example, the loaded UHPC connection will be referred to as specimen U-L.

When labels only include the material and loading identifiers, the connection is being referred to. If an additional letter or number is present, a test specimen is being called out. If this first part includes a "C" preceding the material identifier (i.e., CAA-L), it is referring to a corrosion test

specimen. If a number follows the "AA" or "U" (i.e., U2-N) it is identifying a freeze-thaw test specimen.

3.5 Cyclic Loading

One UHPC joint specimen (U-L) and one AA joint specimen (AA-L) was subjected to cyclic loading. These loadings simulate expected in-service traffic loads. An MTS serve-controlled hydraulic cylinder and load frame located at Fears Lab was utilized for this testing. This machine is designed to apply up to 22,000 pounds of force.

The specimen was placed upside down and loaded to produce tension stresses perpendicular to the joint. This loading was to simulate instances where loads were on the adjacent decks of the connection and no loading was on the link slab. The test loading consisted of 100,000 cycles of 5,000 pounds, which was based on the cracking stress of the link slab for the AA material. The end supports of the specimen during this testing were at the four corners of the specimen. Loading was applied through a steel beam in the middle of the specimen to distribute loading along the joint. Figure 3-25 shows the testing setup for tension loading. After reaching the cycle count, each specimen was inspected for cracking.

Figure 3-25: Cyclic load testing setup for tension on link slab surface

Compression loading applied 20 cycles of 18,000 pounds with the surface face up to simulate traffic loads on the connection. This loading is based on the cracking moment of the AA concrete for the full deck section of 8 in. The end supports of the specimen during testing were along the 6 ft. edge of the specimen. The steel beam was oriented perpendicular to the connection width to promote bending along the connection width. Figure 3-26 shows the testing setup for compression loading. After reaching the cycle count, each specimen was inspected for cracking.

Figure 3-26: Cyclic load testing setup for compression on link slab surface

Specimen U-L was the first to be tested and started under an initial parameter of a higher cycle count at 18,000 pounds of compressive loading. During testing, issues with the testing machine required a change in the factors. Compression testing stopped short of the initial count and was flipped to conduct tension cyclic loading at the now established parameters.

While cyclically loaded under tension, the Class AA specimen (AA-L) developed a significant crack near the center of the connection. Figure 3-27 shows the crack as it was observed during testing. No such cracking developed in specimen U-L.

Figure 3-27: Cracking in AA-L during cyclic loading (annotated)

The remaining UHPC and AA joint specimens (U-N, AA-N, respectively) did not experience cyclic loading. U-L and AA-L are intended to represent in-service link slabs while U-N and AA-N represent newly constructed link slabs that would also serve as a baseline to indicate the effect of loading on the durability of the link slab joint.

4. Freeze-Thaw Cycling and Resonant Frequency Testing

4.1 Introduction

Three test specimens were sectioned from each link slab specimen to undergo freeze-thaw testing. Each specimen was sawcut with desired dimensions of 4 in. by 12 in. in plan and a 3-in. thickness. Specimens were taken from the middle of the connection where the link slab had a consistent 3-in. thickness. This process is documented in Figures 4-1 through 4-3. Three of the twelve specimens (U1-N, AA3-N, AA2-L) had a piece of #4 rebar running along the 12-in. length near the center of the cross section. Figure 4-4 shows an example of this with specimen AA3-N. It was considered to be unlikely that the presence of the reinforcing bar would affect the test results.

Figure 4-1: Cutting specimen sections from link slab

Figure 4-2: Specimen sections with freeze-thaw lengths indicated with marker

Figure 4-3: Cutting freeze-thaw specimen to length

Figure 4-4: End profile of AA3-N with rebar near center (annotated)

For connection specimen AA-L, only one freeze-thaw specimen (AA2-L) was able to be cut close to the desired 12-in. length. The parent specimen experienced cracking close to the 2-inch gap of the link slab joint during cyclic loading. This cracking caused the other two freeze-thaw specimens, which did not have rebar running along their lengths, to break into uneven sections shorter than 12 in. An example of the effects of cracking is shown in Figure 4-5. The resulting lengths of each AA-L specimen are as follows: AA1-L is 6 in., AA2-L is 11 in., and AA3-L is 8 in. The cracking would be expected to affect overall durability, both in this research and during service.

Figure 4-5: Cracking in AA1-N within 12-inch length denoted with marker

4.2 Procedure

Prior to testing, all specimens were fully submerged in a lime water bath for 7 days to ensure

full saturation expected in testing. Testing was in accordance with ASTM C666 and was

conducted in a freeze-thaw cabinet located at Fears Lab. The cabinet houses twelve metal

containers to hold the specimens. One of the containers held a control specimen (Figure 4-6).

Sensors were inserted into the center of this control specimen to monitor the temperature

changes, as the testing cycle temperatures refer to the specimens' internal temperatures. The

wires for these sensors can be seen in Figure 4-6. Cycles took specimens above and below

freezing temperatures at a rate of approximately 3 hours per cycle. The target extreme

temperatures were 40° and 0° Fahrenheit. Testing was conducted for a total of 350 temperature cycles.

Figure 4-6: Control specimen in freeze-thaw tray

Specimens were removed every 36 cycles to determine their resonant frequencies throughout testing. Testing in the freeze-thaw cabinet was stopped between cycles, with the temperature reading 40° Fahrenheit. Once all specimens were completely thawed, they were placed into lime baths in a temperature-controlled room for at least 24 hours before resonant frequency testing. After collecting these readings, specimens were placed back into the freeze-thaw machine for the next series of cycles.

4.3 Testing

The testing setup in the freeze-thaw cabinet is shown in Figure 4-7. Due to only having eleven containers available for testing (with the twelfth container taken by the control specimen), the

shortest specimen, AA1-L, was not tested. After each period of cycling, the specimens were

usually left to thaw overnight; with uneven heating in the machine and testing occurring during

winter, this process took longer than anticipated. Specimens rotated positions in the machine for

each series of cycles to account for this inconsistency. As the specimens cured in lime water

between series of temperature cycles, the water used in the freeze-thaw machine was discarded

and replaced with clean water. A few of the specimens had an uneven underside where the

connected decks were not level when the link slab was cast. To be consistent and avoid any

issues in testing, all specimens were tested in the freeze-thaw cabinet with the level top surface at

the bottom (Figure 4-8). The sheet gasket was not able to be removed from the specimens

completely, resulting in a layer of its residue on each specimen, also shown in Figure 4-8. This

practice was also implemented to collecting frequency readings, with all specimens tested

upside-down.

Figure 4-7: Freeze-thaw specimens thawing in cabinet

Figure 4-8: Standard orientation of specimen placed in freeze-thaw tray

To obtain resonant frequency readings, a specimen was placed on a test bench consisting of a

metal bar for the specimen to balance on with another on top to hold it in place. The testing setup

is shown in Figure 4-9. During a test, one end of the specimen was struck by a steel impactor at

the face's center (for Figure 4-9, the striking end is to the right). The impactor is a 6-in.

pendulum with a weighted steel ball at the end. The ball weighs 0.42 oz and has a diameter of

0.55 in. Figure 4-10 shows the striking instrument. On the other end of the specimen, a miniature accelerometer was placed against the center of the face. This sensor was attached to an emodumeter and read the vibrations when the concrete was struck. The emodumeter then determined and provided the resonant frequency of the concrete specimen. This instrument setup is shown in Figure 4-11. Three readings were collected for each specimen per round of testing. The averaged frequency values were used to calculate the specimen's relative dynamic modulus (RDM) of elasticity. The short specimen being tested, AA3-L, had inconsistent readings throughout testing, so five readings were collected per round.
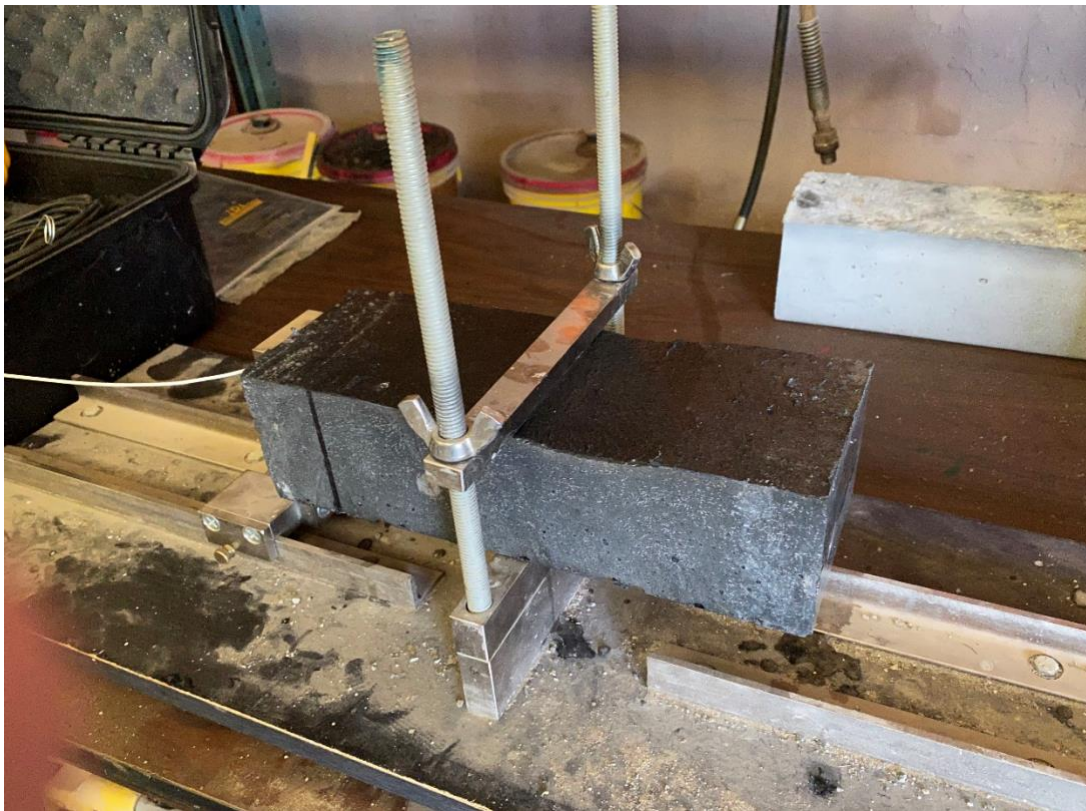
Figure 4-9: Freeze-thaw specimen on test bench to collect frequency readings

Figure 4-10: Steel impactor used to collect frequency readings

Figure 4-11: Emodumeter with accelerometer connected (white wire)

4.4 Summary of Results

The RDM of each freeze-thaw specimen was determined as a squared ratio of the specimen's measured frequency to its initial frequency collected before testing began. This calculation was based on ASTM C666. These values were calculated for each interval resonant frequencies were measured. Figure 4-12 shows a plot of the average RDM values for each specimen type throughout testing. The dramatic dip in value in the first 100 cycles of AA-L is unexpected and may be due to issues in collecting data during testing.
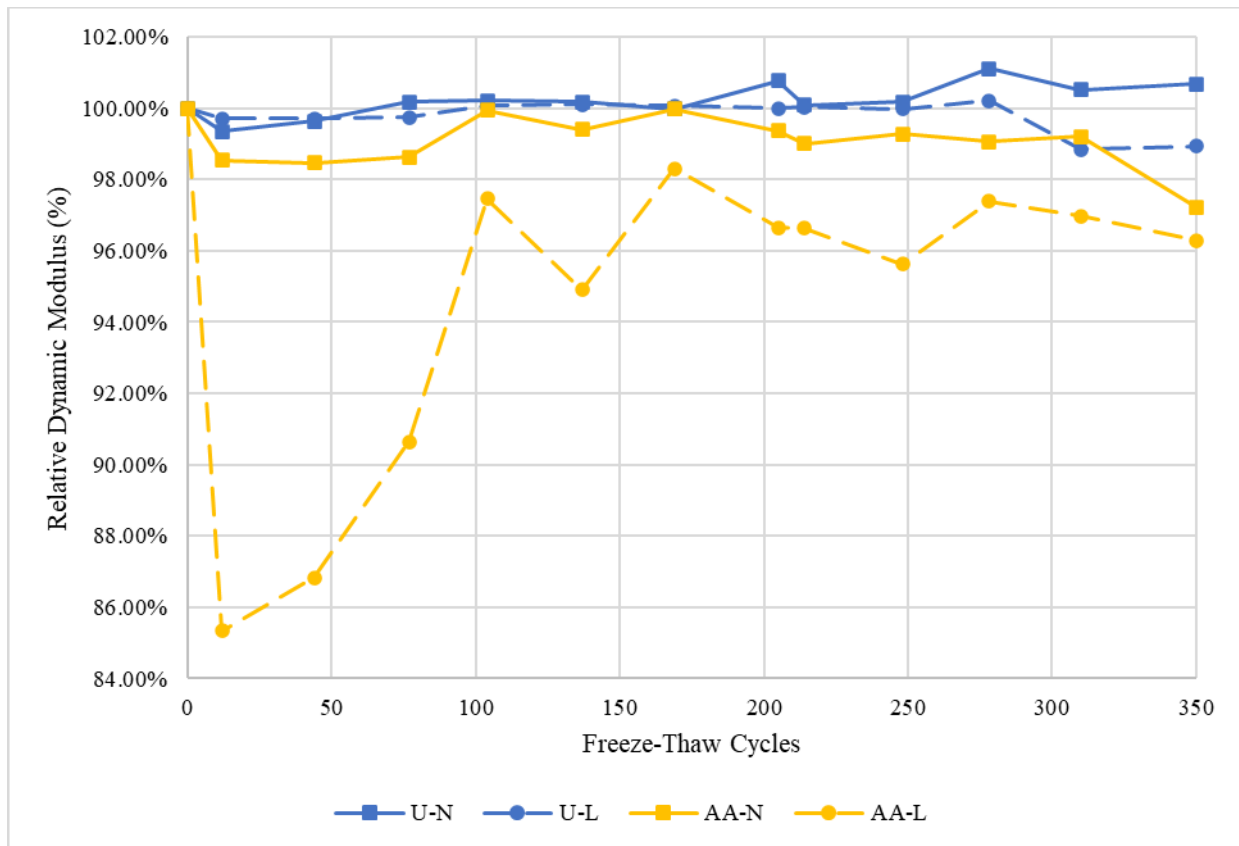
Figure 4-12: Plot of average RDM values for link slab specimens

Overall, the UHPC specimens fared better than the AA specimens. When looking at specimens similarly loaded, this holds true; the J3 specimens retained higher RDM values than AA specimens. Prolonged saturation throughout testing promoted further curing in UHPC specimens with water seeping superficially into the surface of specimens and activating dry cementitious material. This reaction likely caused most of the UHPC specimens to develop slightly higher stiffness by the end of testing. This increase in stiffness is denoted by RDM values greater than 100%. Specimens U3-N and U3-L were the only UHPC specimens to lose strength. Microcracking likely developed during cyclic loading and may have contributed to the relatively significant RDM decrease of U3-L. All AA specimens experienced stiffness loss by some degree, with the loaded specimens AA2-L and AA3-L having the greatest reduction in stiffness. Table 4-1 shows the average RDM for each specimen type at the end of testing, and Table 4-2 lists the average RDM of each specimen after 350 cycles. With specimen AA3-L having a shorter length than what is called for in ASTM C666, frequency readings were inconsistent and were deemed unreliable to include in the plotting of Figure 4-12. The RDM value for AA3-L in Table 4-2 was determined as all other specimen values by excluding outliers and is included for thoroughness. This exclusion made specimen AA2-L the only representing specimen for link slab AA-L in Figure 4-12 and Table 4-1. The measured frequencies throughout testing for all specimens are recorded in Tables A-1 through A-4 of the appendix.

Table 4-1: Average RDM values after 350 freeze-thaw cycles

U-N	U-L	AA-N	AA-L
100.68%	98.93%	97.22%	96.28%

Table 4-2: Average RDM readings per specimen after 350 freeze-thaw cycles

Specimen	RDM
U1-N	101.76%
U2-N	100.55%
U3-N	99.72%
U1-L	100.77%
U2-L	100.29%
U3-L	95.85%
AA1-N	93.45%
AA2-N	98.91%
AA3-N	99.28%
AA2-L	96.28%
AA3-L	15.55%

Physical changes were observed and recorded during testing. One specimen from each link slab

is pictured in Figures 4-13 through 4-15 showing the progression of their surface states from

before testing, after 170 cycles, and after 350 cycles when testing concluded. All respective

specimens showed similar changes due to testing. Photos for these figures are of the same

location of each specimen, as best as could have been achieved with the deterioration of

distinguishing marks such as marker labels.
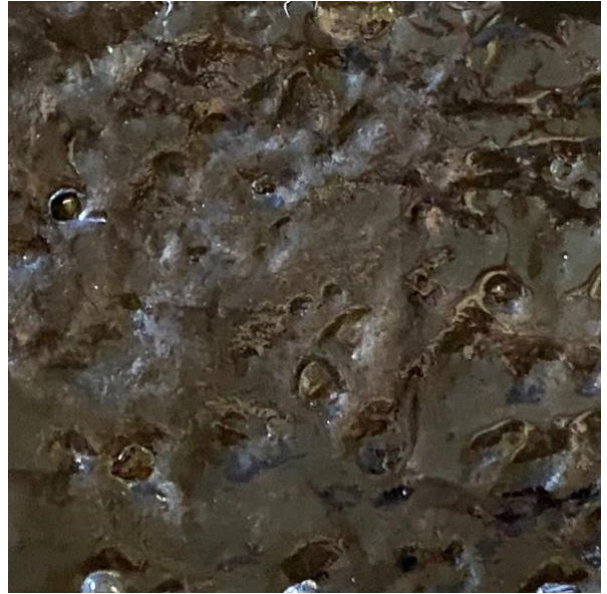
(a)   (b)
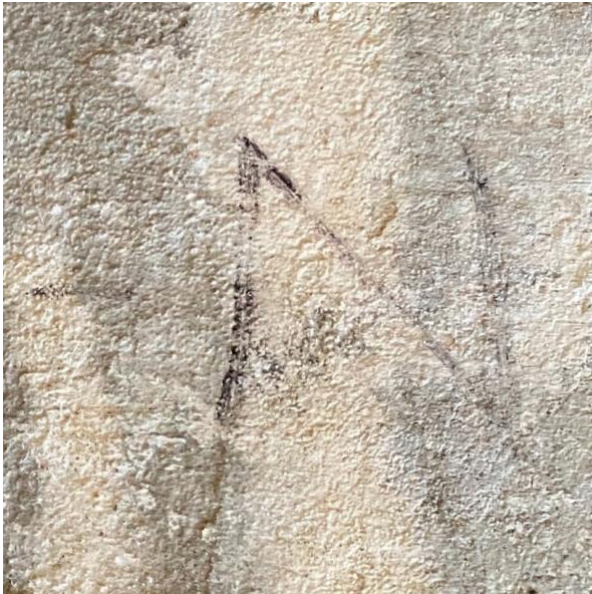
(c)   (d)

Figure 4-13: Surface condition at beginning of testing (0 freeze-thaw cycles) for specimens (a) U2-N, (b) U2-L, (c) AA2-N, (d) AA2-L

(a)

(b)

(c)

(d)

Figure 4-14: Surface condition at 170 freeze-thaw cycles for specimens (a) U2-N, (b) U2-L,
(c) AA2-N, (d) AA2-L
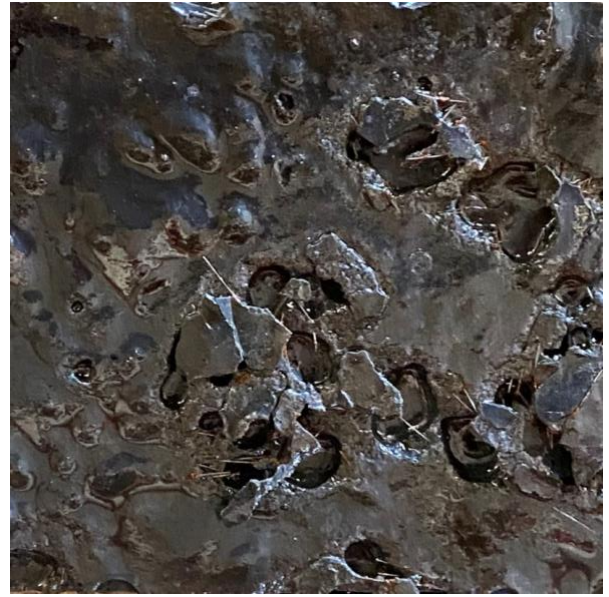
(a)   (b)

(c)   (d)

Figure 4-15: Surface condition at 350 freeze-thaw cycles for specimens (a) U2-N, (b) U2-L, (c) AA2-N, (d) AA2-L

For the U-L, AA-N, and AA-L specimens, varying degrees of scaling developed on the top surface, with the loaded specimens having the more severe scaling. While AA specimens developed this scaling during testing, U-L specimens had preexisting pockets on their surfaces, as shown in Figure 4-13b. Scaling pieces on the U-L specimens were considerably larger than the AA specimens due to the steel fibers present. Mass was not measured during for this test; any discussion of material loss is based on observations. The finer residue from AA specimens is shown in a testing tray during testing in Figure 4-16. Pronounced pockets on UHPC surfaces indicate material loss as well, but not to the degree observed by AA specimens. Furthermore, AA specimens experienced chipped edges. Figures 4-17 through 4-20 show these affected areas. U-N specimens have little to no observable scaling to its surface, demonstrated in Figure 4-15a, while none of the UHPC specimens showed signs of chipping.

Figure 4-16: Concrete residue in tray after removal of specimen AA2-L

Figure 4-17: Chipped corner of specimen AA2-N

Figure 4-18: Chipped edges, face of specimen AA3-N

Figure 4-19: Chipped edges of specimen AA2-L

Figure 4-20: Chipped edges, face of specimen AA3-L

5. Accelerated Corrosion Testing

5.1 Introduction

Accelerated corrosion testing was completed to gauge how well each link slab would perform during actual in-service exposure. As with the freeze-thaw testing, performance was expected to differ between specimens of different material as well as whether the specimens were subjected to cyclic loading. The accelerated corrosion test setup was based on previous research (Abosrra et al., 2011; Leggs, 2019; Wang et al., 2017).

One segment from each of the four link slab specimens was subjected to accelerated corrosion testing. All corrosion specimens were sectioned at the same time as the freeze-thaw specimens. Each specimen for corrosion testing measured 1 ft. by 6 ft. in plan and 8 in. in thickness. Each specimen included one of the copper wires previously soldered to the link slab reinforcing cages during specimen fabrication. The ends of the rebar exposed due to sectioning the link slab specimens were coated with a liquid rubber sealant. This covering was applied to simulate an unaltered link slab specimen, as these rebar ends would not be exposed in an actual deck while in service. Figure 5-1 shows a specimen side with the rubber sealant applied. As a reminder, the "C" in a specimen's label indicates it was subjected to accelerated corrosion testing.

Figure 5-1: Corrosion specimen CU-N with sealant applied to exposed rebar ends

5.2 Procedure

For accelerated corrosion testing, each segment was partially submerged in a 5% saline solution. A receptacle resembling a pool was constructed for each specimen, resulting in four individual containers, one for each specimen. In this case, the formwork from the initial slab construction was recycled as the framing for the pools. Each receptacle was lined with two layers of plastic that was secured in place with heavy duty tape.

Before specimens were placed in the testing pools, they were flipped upside-down to ensure the connection portion was always in contact with the solution, and to mimic the fact that the top surface of the link slab joints would be exposed to road salts and other deleterious materials in an actual bridge. The specimens were then placed in their respective chambers with an overhead crane. A pair of 3/8-in. aluminum bars were used as footings for each specimen and were placed near the specimen ends. This support facilitated placement and removal of the specimens as well as allowing the solution to cover the connection surface. The bars also allowed room for each

54

specimen's copper wire to run up and above the water line without being severed. Liquid rubber sealant was applied on the plastic under the aluminum bars for additional protection for the liner.

The specimens were partially submerged in a 5% saline solution throughout corrosion testing. The percentage refers to salt accounting for 5% of the total weight of the solution. Water was mixed with salt in 100-gallon tubs before being added to the testing pools. Figure 5-2 shows the transfer of the solution by a water pump and hose. Each specimen was submerged approximately 3 in. within the solution.

Figure 5-2: Saline solution transferring to specimen baths

Two DC power supplies were utilized to provide the electric current for corrosion testing. One of the power sources is shown in Figure 5-3 along with the set values of 0.2 amps and 10.0 volts.

The copper wire from each specimen was spliced and connected to the power supply on the positive end of its respective current path. The negative end of each path was wired to a stainless steel rod placed in the solution bath. Throughout testing, an electric current was running through each specimen and solution and maintained at 0.2 amps. Current flow proceeded from the power supply to the stainless steel rod (cathode), then through the saline solution, then through the concrete pore water solution, then through the rebar (anode), and then back to the power supply via the copper wire soldered to the rebar. This testing setup and current flow is depicted in Figure 5-4. The total time for running the accelerated corrosion testing was 9 weeks.

Figure 5-3: DC power supply with test settings
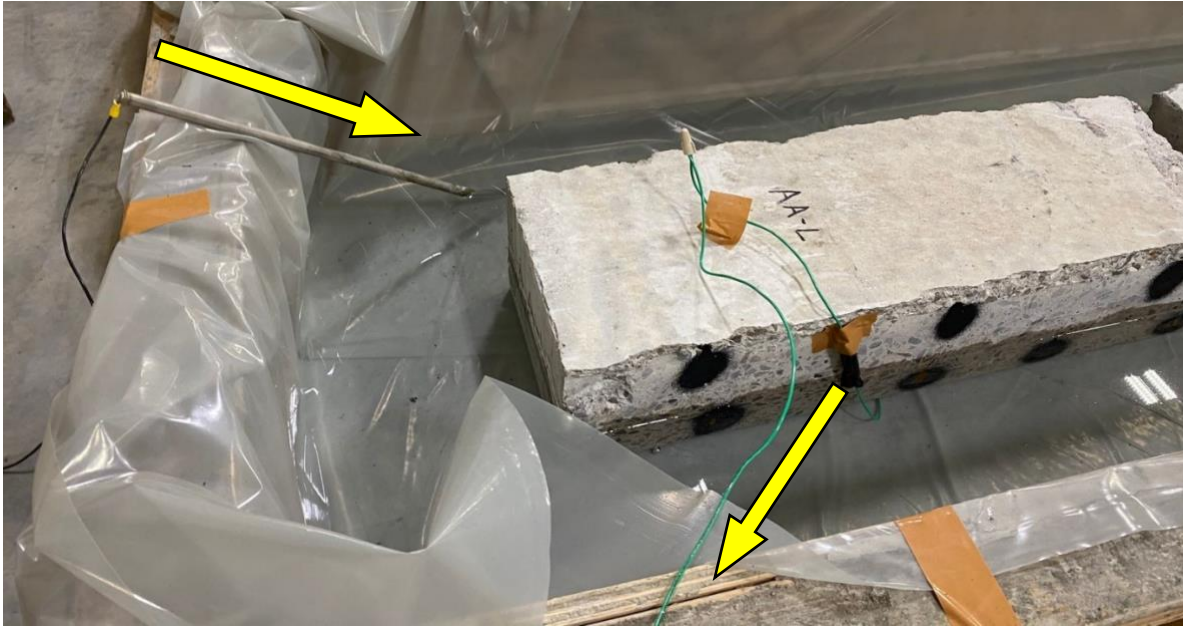
Figure 5-4: Corrosion testing setup and electrical current path

5.3 Testing

The voltage readings indicated on the readout of the power supplies were the returning voltages for each specimen and were recorded periodically. The power supply maintained the current at 0.2 amps. The water level of the solution was monitored, and fresh water was added as needed. No salt was added to maintain the 5% salt-to-water ratio for the saline solution.

After 5 weeks of accelerated corrosion, testing was paused to observe the status of the connection rebar. Specimens were unhooked from the DC power supplies, removed from their pools, and flipped to have the connection surface on top. For each specimen, two windows were cut and chiseled into the surface to expose two pieces of reinforcing steel to view and document any effects of corrosion on the steel or surrounding concrete. Once this data was collected, all

windows were filled with UHPC and cured for 7 days. Epoxy was also applied to the surface of these patches for extra protection.

The rubber sealant initially used to seal the exposed ends of the rebar that resulted from the specimen saw cutting process did not perform as well as envisioned. Consequently, after opening of the windows to observe the condition of the rebar, the exposed ends of the rebar were coated with a two-part epoxy. The specimens were then flipped, placed back into the pools containing new saline solution, and testing resumed for another 4 weeks. After testing concluded, the same process was followed to observe two more segments of rebar in the connection.

5.4 Summary of Results

The returning voltages were recorded periodically throughout testing for all specimens. Figure 5-5 is a plot comparing the voltage readings for each specimen for the duration of testing. Note the break at day 37 when testing was paused and resumed with new saline solution.
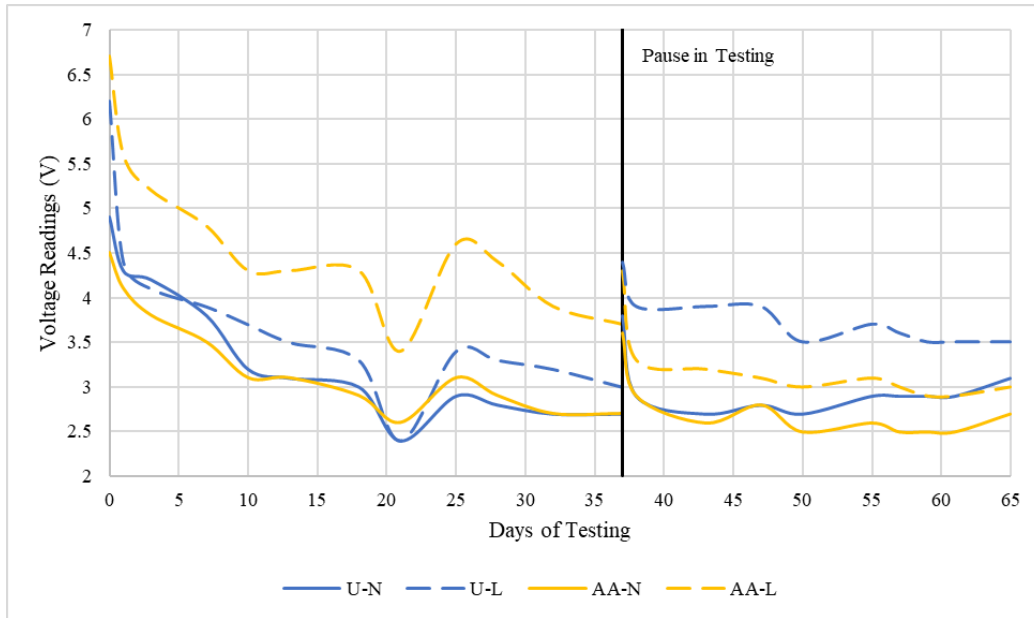
Figure 5-5: Plot comparing corrosion specimen voltage readings during testing

In general, lower voltage readings would indicate increased corrosion potential. Unloaded specimens tended to have similar readings throughout testing, with the highest spread between them being 0.5V at the conclusion of testing. It is unclear why the loaded specimens developed different reading trends after the pause in testing than before. The following figure shows the setup for the accelerated corrosion testing of specimen CU-L through its first 5 weeks. Photos shown in Figure 5-6 were taken at the following time increments: 0 days (when testing began), 3 days, 18 days, and 37 days. All corrosion specimens experienced similar progressions during testing.

(a)   (b)

(c)   (d)

Figure 5-6: Specimen CU-L at (a) the beginning of testing, (b) 3 days of testing, (c) 18 days of testing, and (d) 37 days of testing

After 5 weeks, specimens were removed from the solution baths, flipped, and windows were cut

to observe the state of the reinforcing steel within the link slab connection. Figure 5-7 shows the

surface of specimen CAA-L after being flipped over. The rebar and surrounding concrete

observed in this specimen are shown in Figures 5-8 and 5-9. Cracking in the connection

developed in CAA-L during cyclic loading and is shown in Figure 5-10. Surface cracking raises

the potential for the solution to seep into the connection and initiate premature cracking. Similar

photographs of all other specimens are provided in Figures 5-11 through 5-20. Cracking was also

observed on the surface of CAA-N. The crack coincided with rebar layouts and is corrosion-

induced. No cracking was observed in the UHPC corrosion specimens.

Figure 5-7: Surface of CAA-L after 37 days of testing, windows cut

Figure 5-8: CAA-L observed rebar A, 37 days tested

Figure 5-9: CAA-L observed rebar B, 37 days tested

Figure 5-10: Cracking in specimen CAA-L (present prior to testing, annotated)

Figure 5-11: Surface of CAA-N after 37 days of testing, windows cut

Figure 5-12: CAA-N observed rebar A, 37 days tested

Figure 5-13: CAA-N observed rebar B, 37 days tested

Figure 5-14: Cracking in specimen CAA-N (annotated)

Figure 5-15: Surface of CU-L after 37 days of testing, windows cut

Figure 5-16: CU-L observed rebar A, 37 days tested

68

Figure 5-17: CU-L observed rebar B, 37 days tested

Figure 5-18: Surface of CU-N after 37 days of testing, windows cut

Figure 5-19: CU-N observed rebar A, 37 days tested

Figure 5-20: CU-N observed rebar B, 37 days tested

At this checkpoint, signs of corrosion were evident on and around the rebar in the AA specimens. The surrounding concrete in the window cutouts showed discoloration due to corrosion comparable to what was observed on the specimen surfaces; this is shown prominently in Figures 5-9 and 5-13, The rebar appeared to have also slightly dulled and had begun to oxidize due to corrosion. These characteristics were observed in all window cutouts for Class AA corrosion specimens.

UHPC corrosion specimens fared better within the conditions of the rebar and surrounding concrete. Once the surface was removed for the window cutouts, the underlying concrete of the UHPC link slab specimens were in a significantly better condition, with only traces of discoloration, observed in Figure 5-17, likely due to the presence of steel fibers. The observed conditions of the rebar within the UHPC were also more intact than those observed in the AA specimens, even considering the poor insulation of the liquid rubber sealant. All observed rebar in the UHPC specimens indicated similar results.

Corrosion testing resumed for an additional 28 days on all specimens. Figure 5-21 shows the progression of specimen CU-L in the testing pool at the time testing resumed (37 days), 47 days, 55 days, and 65 days, when testing concluded. All specimens experienced a similar progression.

(a)   (b)

(c)   (d)

Figure 5-21: Specimen CU-L at (a) 37 days of testing, (b) 47 days of testing, (c) 55 days of testing, and (d) 65 days of testing

73

After 65 days of total testing time, the state of the connection rebar was observed in the same process conducted at the 37-day checkpoint. Windows were cut for two more segments of rebar in the link slab. Figures 5-22 through 5-27 show the surface and rebar of the AA specimens. Figures 5-28 through 5-33 show the surface and rebar of the UHPC specimens. As with the status of the rebar and surrounding concrete observed at 37 days of corrosion, the status of the rebar in UHPC specimens fared better than Class AA specimens, regardless of whether they were cyclically loaded prior to testing. The Class AA specimens show no signs of corrosion in the rebar and minor signs in the surrounding concrete are seen in CAA-L (Figure 5-23). Cracking observed previously on AA specimens was more pronounced and is annotated in Figures 5-22 and 5-25, indicating further effects of corrosion. No damage was observed at the patched areas of the first set of windows for any specimen.

Figure 5-22: Surface of specimen CAA-L after 65 days of corrosion testing

Figure 5-23: CAA-L observed rebar C, 65 days tested

Figure 5-24: CAA-L observed rebar D, 65 days tested

Figure 5-25: Surface of specimen CAA-N after 65 days of corrosion testing

Figure 5-26: CAA-N observed rebar C, 65 days tested

Figure 5-27: CAA-N observed rebar D, 65 days tested

Figure 5-28: Surface of specimen CU-L after 65 days of corrosion testing

Figure 5-29: CU-L observed rebar C, 65 days tested

Figure 5-30: CU-L observed rebar D, 65 days tested

Figure 5-31: Surface of specimen CU-N after 65 days of corrosion testing

Figure 5-32: CU-N observed rebar C, 65 days tested

Figure 5-33: CU-N observed rebar D, 65 days tested

6. Findings, Conclusions, and Recommendations

The following chapter summarizes the findings, conclusions, and recommendations from this research study.

6.1 Findings

The following sections cover a list of findings based on test results presented in Chapters 4 and 5.

6.1.1 Freeze-Thaw Cycling and Resonant Frequency Measurements

The following findings were observed during rapid freeze-thaw cycling:

- The majority of the UHPC specimens had an RDM reading greater than 100% after 350 cycles.

- All ODOT Class AA specimens had an RDM reading less than 100% at the conclusion of testing. Specimen AA3-L had inconsistent readings due to its length and possibly due to severe damage and was deemed unreliable to include in results.

- UHPC specimen RDM readings averaged higher than Class AA specimen readings. For both materials, the specimens not subjected to cyclic loading had RDM readings higher than specimens subjected to cyclic loading.

- UHPC specimen surfaces showed little to no signs of scaling or other changes. U-N specimens showed no signs of deterioration. U-L specimens showed surface defects,

though their initial surface state included pockets susceptible to future decline. No

notable signs of chipped edges or faces were observed.

- Class AA specimen surfaces experienced moderate to severe scaling and chipping. AA-L

  specimens had the worst cases of both forms of deterioration. Scaling of AA surfaces

  created concrete residue much finer than what was observed on U-L surfaces.

6.1.2 Accelerated Corrosion Testing

The following findings were observed during accelerated corrosion testing:

- Specimens of link slabs subjected to cyclic loading tended to have higher voltage returns

  during testing than specimens not subjected to cyclic loading. Specimens of non-loaded

  connections tended to have similar voltage returns throughout most of testing, with the

  largest recorded spread of 0.5V after 65 days of corrosion testing.

- After 37 days of corrosion testing, cracks were discovered running along the two

  innermost rebar segments in both Class AA link slab specimens. No similar cracking was

  found in either UHPC specimens.

- Rebar in AA specimens were observed to be in good condition after 37 days of testing,

  with mild signs of oxidation and discoloration in the surrounding concrete. No signs of

  corrosion were found on the rebar or surrounding concrete of UHPC specimens.

- After 65 days of corrosion testing, there were more cracks observed in AA specimens,

  following the same rebar orientations. Previously observed cracks were wider and more

  pronounced. UHPC specimens were observed to have no cracking.

- Rebar observed in AA specimens at 65 days had similar conditions than those observed at 37 days, if not more severe. Signs of oxidation are more apparent on the rebar and the surrounding concrete, especially in the specimen of the link slab subjected to cyclic loading. No signs of corrosion were found on the rebar or surrounding concrete of UHPC specimens.

6.2 Conclusions

The following are conclusions based on findings from freeze-thaw cycling and accelerated corrosion test results:

- Cyclic loading prior to testing had a negative effect on freeze-thaw resistance for both UHPC and ODOT Class AA concrete. Prior loading had a greater effect on Class AA concrete than UHPC.

- UHPC specimens tended to slightly increase in strength during freeze-thaw cycling due to prolonged saturation curing of previously unhydrated cementitious material.

- UHPC was able to withstand surface deterioration better than Class AA concrete during freeze-thaw cycling. Though scaling was observed in U-L specimens, steel fibers held the cracked pieces together and prevented more material loss than observed.

- UHPC provides better protection against deterioration than Class AA concrete in accelerated corrosion testing.

- Prior cyclic loading does affect the performance of Class AA concrete during accelerated corrosion testing, making its reinforcement more susceptible to contaminant contact.

85

- Prior cyclic loading had no observable effect on UHPC's ability to resist corrosion as a link slab connection.

- Class AA concrete is more susceptible to corrosion-induced cracking than UHPC.

- UHPC will provide greater resistance to adverse effects of freeze-thaw cycling and corrosion than ODOT Class AA concrete in a link slab bridge joint.

6.3 Recommendations

Recommendations for future research of UHPC performance in link slab bridge joints are as follows:

- Fabricate all connections of the same material from the same mixing batch for a more consistent and direct comparison of the effects of cyclic loading.

- Conduct alternative forms of corrosion testing where the connection surface would be subjected to a cycling of water and air exposure to simulate comparable weather conditions, such as intermittent rain, during service.

- Investigate how variations in loading conditions may affect UHPC link slab performance.

- Compare UHPC link slabs with varying amounts of steel fibers to see how it may affect its durability, notably in freeze-thaw cycling.

- Conduct similar testing comparing the performance of proprietary UHPC and non-proprietary UHPC mixes, such as the J3 mix.

Appendix

The following tables feature resonant frequency measurements of specimens throughout rapid freeze-thaw cycling. Note the values highlighted were considered outliers and disregarded in determining RDM values.

Table A-1: Resonant frequencies of freeze-thaw specimens at cycles 0-44

Cycle Count:	0			12				44				
U1-N	7109	7109	7109	7109	7109	7109		7119	7119	7119		
U2-N	6973	6973	6973	6924	6924	6924		6973	6973	6973		
U3-N	7061	7061	7061	7041	7041	7041		7012	7012	7012		
U1-L	6787	6787	6787	6777	6777	6777		6787	6787	6787		
U2-L	6836	6836	6836	6826	6826	6826		6816	6816	6816		
U3-L	7012	7012	7012	7002	7002	7002		7002	7002	7002		
AA1-N	7031	7031	7031	6963	6963	6963		6963	6963	6963		
AA2-N	7139	7139	7139	7090	7090	7090		7080	7100	7090		
AA3-N	7148	7148	7148	7109	7109	7109		7100	7100	7100		
AA2-L	6924	6924	6924	6445	6367	6377		6465	6436	6455		
AA3-L*	5166	5156	5264	7070	771	6943	7021	6514	1025	5508	1104	5547

(Specimen Readings (Hz). Highlighted outlier values: 771, 1025, 1104.)

*Specimen AA3-L is 8 in. in length

Table A-2: Resonant frequencies of freeze-thaw specimens at cycles 77 - 170

Cycle Count:	77			105			138				170				
U1-N	7119	7119	7119	7139	7139	7139	7139	7139	7139		7139	7139	7139		
U2-N	6982	6982	6982	6992	7002	7002	6943	6943	6943		6963	6963	6963		
U3-N	7061	7061	7061	7021	7031	7031	7080	7080	7080		7031	7041	7041		
U1-L	6777	6777	6787	6797	6797	6787	6797	6797	6797		6787	6787	6787		
U2-L	6826	6826	6826	6836	6836	6836	6836	6836	6836		6846	6846	6836		
U3-L	7002	7002	7002	7012	7012	7012	7012	7012	7012		7012	7012	7012		
AA1-N	6963	6963	6963	7021	7021	7021	6992	6992	7002		7012	7012	7012		
AA2-N	7109	7100	7100	7139	7139	7139	7109	7119	7119		7148	7139	7148		
AA3-N	7109	7100	7109	7148	7158	7148	7139	7139	7148		7158	7158	7158		
AA2-L	6641	6592	6543	6855	6865	6787	6758	6729	6748		6865	6875	6855		
AA3-L*	4365	2461	5303	1084	1221	1211	3984	1484	1445	1543	1201	4219	723	928	801

(Specimen Readings (Hz). Highlighted outlier values: 2461, 3984, 1201, 4219.)

*Specimen AA3-L is 8 in. in length

Table A-3: Resonant frequencies of freeze-thaw specimens at cycles 206-249

Cycle Count:	206					215					249				
U1-N	7139	7139	7139			7148	7148	7148			7148	7148	7148		
U2-N	7002	7002	7002			6973	6973	6973			7002	6973	6973		
U3-N	7080	7080	7090			7031	7031	7031			7031	7031	7031		
U1-L	6787	6787	6787			6787	6787	6797			6787	6787	6787		
U2-L	6836	6836	6836			6836	6836	6836			6836	6836	6836		
U3-L	7012	7012	7012			7012	7012	7012			7002	7012	7012		
AA1-N	7002	7002	7002			6982	6982	6973			6992	6992	6992		
AA2-N	7109	7109	7109			7090	7100	7100			7109	7119	7119		
AA3-N	7148	7139	7129			7129	7139	7139			7129	7129	7139		
AA2-L	6797	6807	6816			6777	6826	6816			6748	6797	6768		
AA3-L*	518	938	410	391	498	4580	2158	2236	2080	4570	4316	4990	2178	2031	1943

(Row label for the whole block: **Specimen Readings (Hz)**)

*Specimen AA3-L is 8 in. in length

Table A-4: Resonant frequencies of freeze-thaw specimens at cycles 279-350

Cycle Count:	279					311					350				
U1-N	7148	7158	7148			7158	7168	7168			7168	7168	7178		
U2-N	7021	7012	7021			6982	6982	6982			6992	6992	6992		
U3-N	7090	7090	7090			7051	7051	7051			7051	7051	7051		
U1-L	6797	6797	6797			6807	6807	6807			6816	6816	6807		
U2-L	6836	6846	6836			6846	6846	6846			6846	6846	6846		
U3-L	7021	7021	7021			6855	6865	6865			6865	6865	6865		
AA1-N	6992	6982	6992			6992	6992	6992			7002	6592	7002	6592	
AA2-N	7109	7100	7100			7100	7100	7109			7100	7100	7100		
AA3-N	7119	7129	7129			7139	7129	7148			7119	7129	7119		
AA2-L	6846	6816	6836			6865	1463	1240	6895	6846	6807	6807	6768		
AA3-L*	4043	2256	3486	1709	1777	3760	3828	1367	3838	3584	3037	1084	3076	1660	1387

(Row label for the whole block: **Specimen Readings (Hz)**)

*Specimen AA3-L is 8 in. in length

References

Abosrra, L., Ashour, A. F., and Youseffi, M. (2011) "Corrosion of steel reinforcement in concrete of different compressive strengths," *Construction and Building Materials*, 25(10): 3915-3925.

ACI, (2019) *Building Code Requirements of Structural Concrete (ACI 318-19)*, American Concrete Institute, Farmington Hills, MI.

ASTM Standard C666/C666M-15 (2015) "Standard Test Method for Resistance of Concrete to Rapid Freezing and Thawing," ASTM International, West Conshohocken, PA, DOI: 10.1520/C0666_C0666M-15, www.astm.org.

Azizinamini, A., Power, E. H., Myers, G. F., Ozyildirim, H. C., Kine, E. S., Whitmore, D. W., and Mertz, D. R. (2013) "Design Guide for Bridges for Service Life," Washington D.C., The National Academies Press.

Chea, K. S. V. (2020) "Comparative Study of Proprietary and Non-Proprietary Ultra-High Performance Concrete as Partial-Depth Joint Replacement," MS Thesis, University of Oklahoma, Norman, OK.

Floyd, R. W., Volz, J. S., Funderburg, C. K., McDaniel, A. S., Looney, T., Casey, C., and

    Coleman, R. (2018) "Evaluation of Ultra-High Performance Concrete for use in Bridge

    Connections and Repair," Annual Report, Oklahoma Department of Transportation,

    Oklahoma City, OK.

Graybeal, B. (2014) *Design and Construction of Field-Cast UHPC Connections*, FHWA-HRT-

    14-084, Federal Highway Administration, McLean, VA.

Haikal, G., Ramirez, J. A., Jahanshahi, M. R., Villamizar, S., & Abdelaleim, O. (2019). *Link slab*

    details and materials (Joint Transportation Research Program Publication No.

    FHWA/IN/JTRP-2019/10). West Lafayette, IN: Purdue University.

    https://doi.org/10.5703/1288284316920

Leggs, M. (2019) "Evaluation of Durability and Corrosion Behavior of Ultra-High Performance

    Concrete for Use in Bridge Connections and Repair.," MS Thesis, University of

    Oklahoma, Norman, OK.

Russell, H. G. and Graybeal, B. A. (2013) "Ultra-High Performance Concrete: A State-of-the-Art

    Report for the Bridge Community," Final Report, Office of Infrastructure Research &

    Development, McLean, VA.

Scarlata, J. (2017) "UHPC Link Slab Design," Workshop, New York Department of

    Transportation, Albany, NY.

Shafei, B., Taylor, P., Phares, B., Dopko, M., Karim, R., Hajilar, S., and Najimi, M. (2018)
"Material Design and Structural Configuration of Link Slabs for ABC Applications,"
Final Report, Accelerated Bridge Construction University Transportation Center, Miami,
FL.

Wang, L., Yi, J., Zhang, J., Jiang, Y., Zhang, X. (2017) "Effect of corrosion-induced crack on the
bond between strand and concrete," *Construction and Building Materials*, 153: 598-606.